Supplementary Material for:

Estimation of rate coefficients and branching ratios for reactions of organic peroxy radicals for use in automated mechanism construction

Contents

S1 $RONO_2$ from the reactions of RO_2 with NO

As discussed in Sect. 2.1 of the main paper, the following two channels are considered for the reactions of RO_2 with NO:

$$RO_2 + NO \rightarrow RO + NO_2 \qquad (S1a)$$

$$\rightarrow RONO_2 \qquad (S1b)$$

The fraction of the reaction forming a nitrate product ($RONO_2$) via the terminating channel (S1b) is denoted R_{1b} (= $k_{1b}/(k_{1a}+k_{1b})$), with the fraction proceeding via the propagating channel (S1a) being R_{1a} (= $k_{1a}/(k_{1a}+k_{1b})$) = $1-R_{1b}$.

Based on the method of Arey et al. (2001), and adopting terminology from Orlando and Tyndall (2012), the reference branching ratio for secondary alkyl peroxy radicals, $R° = (k_{1b}/k_{1a})°$ is calculated as follows:

$$R° = [A/(1 + (A/B))].F^{z} \qquad (i)$$

with $A = 2 \times 10^{-22}.\exp(n_{CON}).[M].(T/300)$, $B = 0.43.(T/300)^{-8}$, F = 0.41, and $z = (1 + (\log_{10}(A/B))^2)^{-1}$.

n_{CON} is the number of carbon oxygen and nitrogen atoms in the organic group of the peroxy radical (equivalent to the carbon number in alkyl peroxy radicals), T is the temperature (in K) and [M] is the gas density (in molecule cm^{-3}).

The fractions of the reaction proceeding via the terminating channel, R_{1b}, and the propagating channel, R_{1a} (= $1-R_{1b}$), for a specific peroxy radical are then given by:

$$R_{1b} = f_a.f_b.R°/(1+R°) \qquad (ii)$$

with the scaling factors, f_a and f_b, introduced here to allow for systematic variations in the yields of $RONO_2$ for primary, secondary and tertiary radicals (f_a), and for the presence of oxygenated functional groups (f_b) (as shown in Tables 2 and 3 of the main paper). Note that a value of f_b needs to be applied to account for the effect of each relevant substituent. Some examples of the method are given below.

Example A: OH + methyl vinyl ketone

The peroxy radicals formed from the reaction of OH with methyl vinyl ketone are predicted to be formed with yields shown below, based on the methods described in Jenkin et al. (2018a):

(1) $CH_2(OH)CH(O_2)C(=O)CH_3$:	78.5 %
(2) $CH_2(O_2)CH(OH)C(=O)CH_3$:	20.9 %
(3) $CH_2=CHC(=O)CH_2O_2$:	0.7 %

The corresponding nitrate yields are calculated as follows:

Radical (1) (yield 0.785)

$n_{CON} = 6$, leading to $R° = 0.196$ at 298 K and 760 Torr.

$f_a = 1.0$ (secondary peroxy radical)

f_b (-C-C(OH)<) = 0.65, and f_b (-C-C(=O)-) = 0.3 need to be applied.

$R_{1b} = 1.0 \times (0.65 \times 0.3) \times 0.196/(1 + 0.196) = 0.0320$; and $R_{1a} = 0.9680$.

Calculated nitrate yield = $0.0320 \times 0.785 = 0.0251$.

Reported nitrate yield = 0.024 ± 0.004 (Praske et al., 2015, at 296 K and 745 Torr).

Radical (2) (yield 0.209)

n_{CON} = 6, leading to $R°$ = 0.196 at 298 K and 760 Torr.

f_a = 0.65 (primary peroxy radical)

f_b (-C-C(OH)<) = 0.65 needs to be applied.

$R_{1b} = 0.65 \times 0.65 \times 0.196/(1 + 0.196) = 0.0692$; and R_{1a} = 0.9308.

Calculated nitrate yield = $0.0692 \times 0.209 = 0.0145$.

Reported nitrate yield = 0.014 ± 0.004 (Praske et al., 2015, at 296 K and 745 Torr).

Radical (3) (yield 0.007)

n_{CON} = 5, leading to $R°$ = 0.119 at 298 K and 760 Torr.

f_a = 0.65 (primary peroxy radical)

f_b (-C-C(=O)-) = 0.3 needs to be applied.

$R_{1b} = 0.65 \times 0.3 \times 0.119/(1 + 0.119) = 0.0207$; and R_{1a} = 0.9793.

Calculated nitrate yield = $0.0207 \times 0.007 = 0.00014$.

Example B: OH + toluene

The hydroxy-dioxa-bicyclo peroxy radicals formed from the addition of OH to toluene are predicted to be formed with yields shown below, based on the methods described in Jenkin et al. (2018b):

(1)

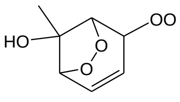

3.5 %

(2)

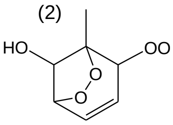

21.1 %

(3)

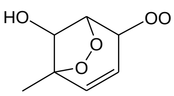

7.0 %

(4)

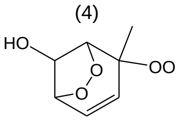

4.5 %

(5)

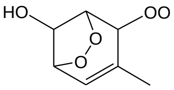

16.1 %

The corresponding nitrate yields are calculated as follows:

Radical (1) (yield 0.035)

n_{CON} = 10, leading to $R°$ = 0.395 at 298 K and 760 Torr.

f_a = 1.0 (secondary hydroxy-dioxa-bicyclo peroxy radical)

f_b = 0.33 (hydroxy-dioxa-bicyclo peroxy radical) needs to be applied.

$R_{1b} = 1.0 \times 0.33 \times 0.395/(1 + 0.395) = 0.0934$; and R_{1a} = 0.9066.

Calculated nitrate yield = $0.0934 \times 0.035 = 0.00327$.

Radical (2) (yield 0.211)

n_{CON} = 10, leading to $R°$ = 0.395 at 298 K and 760 Torr.

f_a = 0.43 (secondary hydroxy-dioxa-bicyclo peroxy radical with adjacent alkyl substituent)

f_b = 0.33 (hydroxy-dioxa-bicyclo peroxy radical) needs to be applied.

$R_{1b} = 0.43 \times 0.33 \times 0.395/(1 + 0.395) = 0.0402$; and R_{1a} = 0.9598.

Calculated nitrate yield = $0.0402 \times 0.211 = 0.00848$.

Radical (3) (yield 0.070)

n_{CON} = 10, leading to R° = 0.395 at 298 K and 760 Torr.

f_{a} = 1.0 (secondary hydroxy-dioxa-bicyclo peroxy radical)

f_{b} = 0.33 (hydroxy-dioxa-bicyclo peroxy radical) needs to be applied.

$R_{1\mathrm{b}} = 1.0 \times 0.33 \times 0.395/(1 + 0.395) = 0.0934$; and $R_{1\mathrm{a}} = 0.9066$.

Calculated nitrate yield = $0.\ 0934 \times 0.070 = 0.00654$.

Radical (4) (yield 0.045)

n_{CON} = 10, leading to R° = 0.395 at 298 K and 760 Torr.

f_{a} = 0.13 (tertiary hydroxy-dioxa-bicyclo peroxy radical)

f_{b} = 0.33 (hydroxy-dioxa-bicyclo peroxy radical) needs to be applied.

$R_{1\mathrm{b}} = 0.13 \times 0.33 \times 0.395/(1 + 0.395) = 0.0121$; and $R_{1\mathrm{a}} = 0.9879$.

Calculated nitrate yield = $0.\ 0121 \times 0.045 = 0.00054$.

Radical (5) (yield 0.161)

n_{CON} = 10, leading to R° = 0.395 at 298 K and 760 Torr.

f_{a} = 1.0 (secondary hydroxy-dioxa-bicyclo peroxy radical)

f_{b} = 0.33 (hydroxy-dioxa-bicyclo peroxy radical) needs to be applied.

$R_{1\mathrm{b}} = 1.0 \times 0.33 \times 0.395/(1 + 0.395) = 0.0934$; and $R_{1\mathrm{a}} = 0.9066$.

Calculated nitrate yield = $0.0934 \times 0.161 = 0.01504$.

The total calculated yield of hydroxy-dioxa-bicyclo nitrates, 3.39 % (at 298 K and 760 Torr), can be compared with the observed yield, 2.9 %, reported by Elrod (2011) (measured at 296-298 K and 200 Torr, but reported to be applicable to 760 Torr).

Example C: OH + *p*-xylene

The hydroxy-dioxa-bicyclo peroxy radicals formed from the addition of OH to *p*-xylene are predicted to be formed with yields shown below, based on the methods described in Jenkin et al. (2018b):

(1)

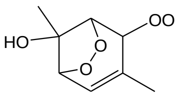

21.0 %

(2)

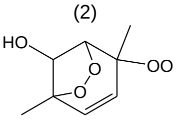

35.5 %

The corresponding nitrate yields are calculated as follows:

Radical (1) (yield 0.210)

n_{CON} = 11, leading to R° = 0.410 at 298 K and 760 Torr.

f_{a} = 1.0 (secondary hydroxy-dioxa-bicyclo peroxy radical)

f_{b} = 0.33 (hydroxy-dioxa-bicyclo peroxy radical) needs to be applied.

$R_{1\mathrm{b}} = 1.0 \times 0.33 \times 0.410/(1 + 0.410) = 0.0960$; and $R_{1\mathrm{a}} = 0.9040$.

Calculated nitrate yield = $0.0960 \times 0.210 = 0.02016$.

Radical (2) (yield 0.355)

n_{CON} = 11, leading to $R°$ = 0.410 at 298 K and 760 Torr.

f_a = 0.13 (tertiary hydroxy-dioxa-bicyclo peroxy radical)

f_b = 0.33 (hydroxy-dioxa-bicyclo peroxy radical) needs to be applied.

$R_{1b} = 0.13 \times 0.33 \times 0.410/(1 + 0.410) = 0.0125$; and $R_{1a} = 0.9875$.

Calculated nitrate yield = $0.0125 \times 0.355 = 0.00444$.

The total calculated yield of hydroxy-dioxa-bicyclo nitrates, 2.46 % (at 298 K and 760 Torr), can be compared with the observed yield, 2.5 %, reported by Elrod (2011) (measured at 296-298 K and 200 Torr, but reported to be applicable to 760 Torr).

S2 Chemically activated RO* radicals from the reactions of RO_2 with NO

As indicated in Sect. 2.1 of the main paper, channel (R2a) is significantly exothermic, such that prompt decomposition (or isomerization) of a fraction of the initially-formed chemically activated oxy radicals, RO*, has been reported to occur in some cases; with the remainder being collisionally deactivated to form thermalized RO (e.g. Orlando et al., 2003; Calvert et al., 2015):

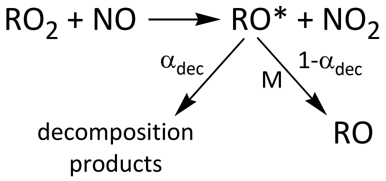

This is has been reported to be particularly important for a number of C_2-C_6 oxygenated oxy radicals and halogenated oxy radicals (e.g. Orlando et al., 2003; Calvert et al., 2015; and references therein), although the latter class is outside the scope of the present study.

Table S1 summarizes the data that form the basis of the prompt decomposition fractions (α_{dec}) applied to chemically activated oxygenated RO* radicals in the present work. The most systematic information is available for primary β-hydroxy oxy radicals of general formula R'CH(OH)CH_2O*, with prompt decomposition fractions at 298 K and 760 Torr reported for the β-C-C bond scission reactions of C_2-C_6 radicals in the theoretical study of Caralp et al. (2003). As shown in Table. S1 and Fig. S1, α_{dec} was calculated to decrease from a value of 0.75 for R' = CH_3 to 0.32 for R'= n-C_4H_9, this being due to a systematic increase in the collisional energy loss with size from the corresponding ROONO intermediates (Caralp et al., 2003). The values of α_{dec} reported for the β-C-C bond scission reactions for the secondary β-hydroxy oxy radical, $HOCH_2CH(O^*)CH_3$, and the primary β-oxo oxy radical, $CH_3C(=O)CH_2O^*$, are similar to that for $CH_3CH(OH)CH_2O^*$, these radicals all possessing the same number of heavy atoms, n_{CON} = 4. It is therefore assumed in the present work that all primary, secondary and tertiary β-hydroxy and β-oxo RO* radicals are characterized by the same size-dependent values of α_{dec} for the β-C-C bond scission reaction as follows,

$\alpha_{dec} = 1.34 - 0.145.n_{CON}$, for $4 \leq n_{CON} \leq 9$;

$\alpha_{dec} = 0$, for $n_{CON} > 9$.

based on the regression of the data for primary R'CH(OH)CH_2O* radicals shown in Fig. S1. For the unique case of $HOCH_2CH_2O^*$ (n_{CON} = 3), a value of α_{dec}= 0.31 is applied, based the average of reported experimental and theoretical values (see Table S1). A number of studies have shown that, where characterized, the values of α_{dec} increase with decreasing pressure and decrease with decreasing temperature (e.g. Vereecken and Peeters, 1999; Vereecken et al., 1999; Orlando et al., 2000). However, these effects therefore tend to compensate each other over the tropospheric range of conditions (e.g. see values for $CH_3C(=O)CH_2O^*$ reported by Orlando et al., 2000). The above values, based on 298 K and

760 Torr data, are therefore assumed here to provide a reasonable estimate for all tropospheric conditions, for simplicity.

Caralp et al. (2003) have also estimated that small fractions (typically < 4 %) of C_4-C_6 primary β-hydroxy RO* radicals may also undergo prompt 1,5 H-shift isomerization reactions. However, because these contributions are minor, and also because 1,5 H-shift isomerization tends to be the major fate of the corresponding thermalized RO radicals, isomerization of β-hydroxy RO* is not represented in the present work.

The studies of Christensen et al. (2000) and Wallington et al. (2001) have established that the α-acyloxy RO* radicals formed during the oxidation of methyl formate and methyl acetate undergo prompt isomerization/decomposition via the α-ester rearrangement mechanism. The reported values of α_{dec} = 0.12 and α_{dec} = 0.20 are thus applied to $HC(=O)OCH_2O^*$ and $CH_3C(=O)OCH_2O^*$, respectively (see Table S1). Although the corresponding process is available (in principle) for other primary and secondary acyloxy RO* radicals, it is likely that the values of α_{dec} are smaller for these larger species, as discussed above for β-hydroxy RO* radicals. Prompt isomerization/decomposition is therefore not generally represented for acyloxy RO* in the present work.

Relatively small effects have also been reported for some C_4 and C_5 unsubstituted alkoxy radicals (Geiger et al., 2002; Libuda et al., 2002; Caralp and Forst, 2003; Cassanelli et al., 2005), as also discussed by Calvert at al. (2015). At present, there is no systematic basis for representing these small effects for unsubstituted alkoxy radicals, and it is anticipated that the effective values of α_{dec} will in any case decrease to close to zero for larger species. It is also noted that Caralp et al. (2008) have subsequently reported a reinterpretation of the observed effects for these unsubstituted systems, not involving fractional prompt decomposition of chemically activated alkoxy radicals.

Table S1. Reported fractions (α_{dec}) of oxygenated RO* radicals formed from RO_2 + NO reactions that undergo prompt decomposition at temperatures near 298 K and pressures near 760 Torr.

n_{CON}	RO*	Products	α_{dec}	Comment
Primary β-hydroxy ($R'CH(OH)CH_2O^*$) [a]				
3	$HOCH_2CH_2O^*$	$CH_2OH + HCHO$	0.31	(c)
4	$CH_3CH(OH)CH_2O^*$	$CH_3CHOH + HCHO$	0.75	(d)
5	$C_2H_5CH(OH)CH_2O^*$	$C_2H_5CHOH + HCHO$	0.63	(d)
6	n-$C_3H_7CH(OH)CH_2O^*$	n-$C_3H_7CHOH + HCHO$	0.47	(d)
7	n-$C_4H_9CH(OH)CH_2O^*$	n-$C_4H_9CHOH + HCHO$	0.32	(d)
Secondary β-hydroxy ($R'CH(OH)CH(O^*)R''$) [a]				
4	$HOCH_2CH(O^*)CH_3$	$CH_2OH + CH_3CHO$	0.775	(e)
Primary β-oxo ($R'C(=O)CH_2O^*$) [a]				
4	$CH_3C(=O)CH_2O^*$	$CH_3CO + HCHO$	0.80	(f)
Primary α-acyloxy ($R'C(=O)OCH_2O^*$) [b]				
4	$HC(O)OCH_2O^*$	$HCOOH + HCO$	0.12 ± 0.03	(g)
5	$CH_3C(O)OCH_2O^*$	$CH_3C(O)OH + HCO$	0.20 ± 0.08	(h)

Comments

[a] Decomposition via β-C-C scission to form products shown; [b] Isomerization/decomposition via α-ester rearrangement to form products shown; [c] Taken from Orlando et al. (2003), based on studies of Orlando et al. (1998), Vereecken and Peeters (1999) and Caralp et al. (2003); [d] Taken from Orlando et al. (2003), based on study of Caralp et al. (2003); [e] Taken from Orlando et al. (2003), based on studies of Vereecken et al. (1999) and Caralp et al. (2003); [f] Based on Orlando et al. (2000); [g] Based on Wallington et al. (2001); [h] Based on Christensen et al. (2000).

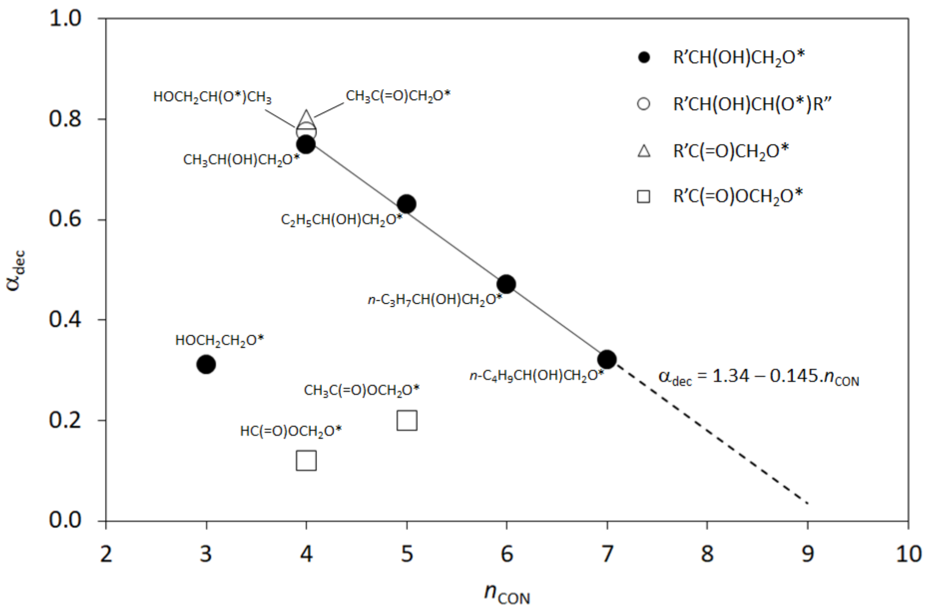

Fig. S1. Prompt decomposition fractions (α_{dec}) for oxygenated RO* radicals formed from RO_2 + NO reactions as a function of n_{CON} at temperatures near 298 K and pressures near 760 Torr.

S3 Fate of ROOOH formed from the reactions of RO$_2$ with OH

As discussed in Sect. 2.4 of the main paper, the reactions of RO_2 radicals with OH form thermalized hydrotrioxides (ROOOH) as major products under atmospheric conditions. Further experimental and theoretical studies are required for the fate of ROOOH under atmospheric conditions to be fully assessed, but information provided in the theoretical studies of Müller et al. (2016), Assaf et al. (2018) and Anglada and Solé (2018) provides some provisional guidance. Based on those studies, the following interim assumptions are applied in the current work:

Thermal decomposition: ROOOH is assumed to decompose via the following channels, with k_{2a}/k_2 = 0.8 and k_{2b}/k_2 = 0.2, based on the calculations of Müller et al. (2016) for CH_3OOOH:

$$\text{ROOOH} \rightarrow \text{RO} + HO_2 \qquad \text{(S2a)}$$

$$\rightarrow \text{ROH} + O_2 \qquad \text{(S2b)}$$

The overall decomposition rate is given by the expression $k_2 = 1.9 \times 10^{10}\ T^{1.35}\ \exp(-12000/T)\ s^{-1}$, as estimated by Assaf et al. (2018). This leads to a decomposition lifetime of about 2 hours at 298 K, increasing to about 8 months at 250 K.

Reaction with OH radicals: The reaction of OH with ROOOH is expected to occur significantly by initial addition to the OOOH group, leading to overall H-atom abstraction and decomposition as follows:

$$\text{OH} + \text{ROOOH} \rightarrow \text{RO} + O_2 + H_2O \qquad \text{(S3)}$$

Based on the calculations of Anglada and Solé (2018) for CH_3OOOH, the rate coefficient is assigned the expression $k_3 = 1.46 \times 10^{-12}\ \exp(1037/T)\ cm^3\ molecule^{-1}\ s^{-1}$, consistent with a lifetime of about 6 hours with respect to this reaction at 298 K, decreasing to about 3 hours at 250 K (for [OH] = 10^6 $molecule^{-1}\ cm^{-3}$). Although calculated to be very minor for CH_3OOOH (Anglada et al., 2018), H-atom abstraction from, or OH addition to, the organic group (R) is likely to be significant for larger and more complex species and needs to be taken into account. The rate coefficient for reaction at the R group is estimated using the SAR methods in the companion papers (Jenkin et al., 2018a; 2018b), with the impact of the OOOH substituent assumed to be the same as that of an OOH substituent, where relevant. For simplicity in this provisional method, however, the total calculated rate coefficient for reaction at R and OOOH is currently applied to reaction (S3).

Other fates: As discussed by Müller et al. (2016) and Assaf et al. (2018), ROOOH is also expected to transfer efficiently to the aqueous phase, or form complexes with water or water clusters, where it likely decomposes to form ROH and O_2. Such processes are outside the scope of the present work, but further information on the phase transfer and multiphase chemistry of ROOOH is clearly required.

S4 Temperature dependence of the reaction of $CH_3C(O)O_2$ with HO_2

As discussed in Sect. 2.5 of the main paper, the following three channels are considered for the reaction of $CH_3C(O)O_2$ with HO_2:

$$CH_3C(O)O_2 + HO_2 \rightarrow CH_3C(O)OOH + O_2 \qquad \text{(S4a)}$$

$$\rightarrow CH_3C(O)OH + O_3 \qquad \text{(S4b)}$$

$$\rightarrow CH_3C(O)O + OH + O_2 \qquad \text{(S4c)}$$

The contribution of the propagating channel (S4c) has been quantified at 293-298 K in a number of more recent studies (Hasson et al., 2004; Jenkin et al., 2007; Dillon and Crowley, 2008; Groß et al., 2014; Winiberg et al., 2016), and a value of k_{4c}/k_4 = 0.5 is assigned at 298 K, based on the average of these determinations. The participation of the terminating channels (S4a) and (S4b) is very well established. Reasonably consistent branching ratios (k_{4a}/k_{4b}), lying in the approximate range 2-3 at room temperature, have been reported in studies where products of both channels have been measured (Niki et al., 1985; Horie and Moortgat, 1992; Hasson et al., 2004; Jenkin et al., 2007; Winiberg et al., 2016), with an average value of 2.8. In conjunction with the above value of k_{4c}/k_4 = 0.5, this results in k_{4a}/k_4 = 0.37 and k_{4b}/k_4 = 0.13 at 298 K.

The temperature dependence of k_{4a}/k_{4b} is defined using the experimental characterization of the reaction reported by Horie and Moortgat (1992), leading to $k_{4a}/k_{4b} = 3.4 \times 10^2 \exp(-1430/T)$. In the absence of laboratory temperature dependence studies of channel (S4c), the temperature dependence of k_{4c}/k_{4b} is based on the results of the theoretical calculations of Hasson et al. (2005) at 250 K and 298 K and atmospheric pressure, leading to the expression $k_{4c}/k_{4b} = 2.34 \times 10^4 \exp(-2600/T)$. The resultant temperature dependent values of the channel contributions (k_{4a}/k_4, k_{4b}/k_4 and k_{4c}/k_4) are given in Table S2 and Fig. S2 (solid lines) for the temperature range 250-300 K.

The value assigned to k_4 at 298 K (= 2.2×10^{-11} cm^3 molecule^{-1} s^{-1}) is based on the average the more recent room temperature kinetics determinations of Groß et al. (2014) and Winiberg et al. (2016), which took account of (and quantified) the importance of channel (S4c) in their analyses. The measurements of k_4 in earlier temperature dependence studies (Atkinson et al., 2006; and references therein) are expected to be subject to systematic errors, because reagent radical regeneration via channel (S4c) was not taken into account in the analyses. Assuming that those studies were effectively partially “blind” to channel (S4c), comparison of the value of k_4 at 298 K with that recommended previously by Atkinson et al. (2006) when channel (S4c) was not taken into account (1.4×10^{-11} cm^3 molecule^{-1} s^{-1}) suggests that the measured value included only 26.7 % of channel (S4c). Making the approximation that the same is true across the temperature range 250-300 K, the temperature dependence recommended by Atkinson et al. (2006), E/R = -980 K, is corrected using the temperature-dependent branching ratios (Table S2), resulting in a revised value of E/R = -580 K (see illustration in Fig. S3). This leads to the temperature dependence expression, $k_4 = 3.14 \times 10^{-12} \exp(580/T)$, as assigned in the present work.

This treatment of the kinetics and product channel branching ratios for the reaction of $CH_3C(O)O_2$ with HO_2 is also applied more generally to the reactions of non-phenyl acyl peroxy radicals with HO_2 in the present work (see Sect. 2.5 of the main paper).

Table S2. Product channel branching ratios, k_{4a}/k_4, k_{4b}/k_4 and k_{4c}/k_4, for the reaction of $CH_3C(O)O_2$ with HO_2 as a function of temperature, based on the method described in Sect. S4.

T (K)	**k_{4a}/k_4 [a]**	**k_{4b}/k_4 [b]**	**k_{4c}/k_4 [c]**
250	0.394	0.354	0.252
255	0.400	0.320	0.280
260	0.403	0.290	0.308
265	0.403	0.261	0.335
270	0.402	0.236	0.363
275	0.398	0.212	0.389
280	0.394	0.191	0.415
285	0.388	0.172	0.440
290	0.381	0.155	0.464
295	0.373	0.140	0.487
298	0.368	0.132	0.500
300	0.365	0.126	0.509

Comments

[a] $k_{4a}/k_4 = (k_{4a}/k_{4b})/(1+ (k_{4a}/k_{4b}) + (k_{4c}/k_{4b}))$; [b] $k_{4b}/k_4 = 1/(1+ (k_{4a}/k_{4b}) + (k_{4c}/k_{4b}))$; [c] $k_{4c}/k_4 = (k_{4c}/k_{4b})/(1+ (k_{4a}/k_{4b}) + (k_{4c}/k_{4b}))$.

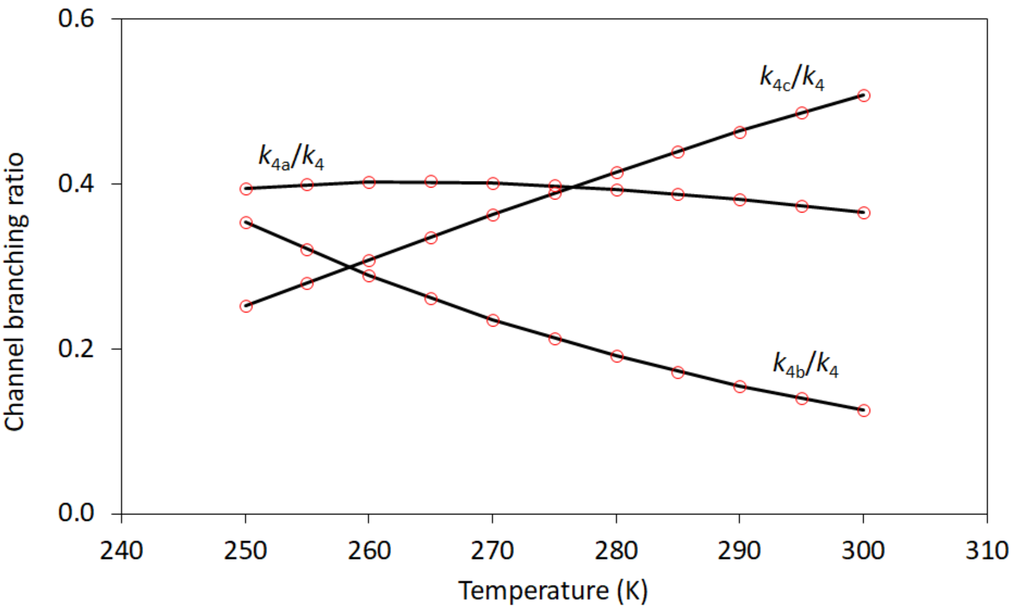

Fig. S2. Temperature dependence of the product channel branching ratios k_{4a}/k_4, k_{4b}/k_4 and k_{4c}/k_4. The solid lines represent the main method described in Sect. S4. The red points are values derived from the individual Arrhenius expressions for k_{4a}, k_{4b} and k_{4c} given in Sect. S4.

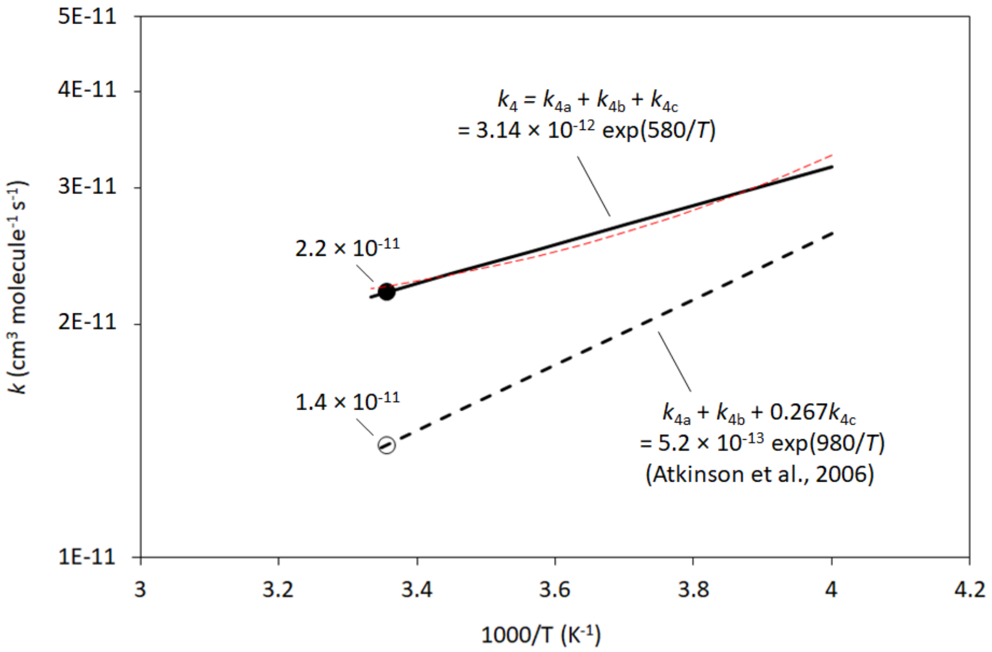

<u>Fig. S3</u>. Illustration of the correction of the previous temperature dependence expression for k_4 (Atkinson et al., 2006) to allow for partial reagent radical regeneration from channel (S4c) (see Sect. S4). The red broken line shows the values of k_4 derived from the individual Arrhenius expressions for k_{4a}, k_{4b} and k_{4c} given in Sect. S4.

It is recognized that the use of temperature-dependent branching ratios in mechanism application can result in computational difficulties. The following expressions are therefore alternative Arrhenius fits to the individual channel rate coefficients derived from the recommended expression for k_4 in conjunction with the temperature-dependent branching ratios for the temperature range 250-300 K:

$k_{4a} = 7.53 \times 10^{-13} \exp(-714/T)$

$k_{4b} = 2.23 \times 10^{-15} \exp(-2142/T)$

$k_{4c} = 5.19 \times 10^{-11} \exp(457/T)$

The use of these expressions results in effective branching ratios that are indistinguishable from those given above (see Fig. S2). As shown in Fig. S3, the total rate coefficients also agree with the recommended expression to within 4 % over the temperature range 250-300 K, although larger deviations would occur if the methods are applied outside this recommended temperature range.

S5 The permutation reactions of RO$_2$

Estimation of self- and cross-reaction rate coefficients: As discussed in Sect. 2.6 of the main paper, the “permutation” reactions of a given RO$_2$ radical are its self-reaction (S5), and its cross-reactions (S6) with other peroxy radicals, R’O$_2$, for which a number of product channels may occur:

$RO_2 + RO_2 \rightarrow RO + RO + O_2$ (S5a)

$\rightarrow R_{-H}O + ROH + O_2$ (S5b)

$\rightarrow ROOR + O_2$ (S5c)

$RO_2 + R'O_2 \rightarrow RO + R'O + O_2$ (S6a)

$\rightarrow R_{-H}O + R'OH + O_2$ (S6b)

$\rightarrow R'_{-H}O + ROH + O_2$ (S6c)

$\rightarrow ROOR' + O_2$ (S6d)

The method used to assign self-reaction rate coefficients (denoted k_{RO2RO2}) to hydrocarbon and oxygenated RO_2 radicals is described in Sect. 2.6. This takes account of the reported activating effects of a number of functional groups (allyl-, benzyl-, hydroxy-, alkoxy-, oxo- and acyl-); the reported trend of decreasing reactivity, primary > secondary > tertiary, for peroxy radicals containing otherwise similar functionalities; and the influence of radical size. As also described in Sect. 2.6, the cross-reaction rate coefficients are mainly inferred from the geometric mean of the rate coefficients for the self-reactions of the participating peroxy radicals; with the exception of reactions involving acyl peroxy radicals, which are assigned a single rate coefficient expression.

Single-class peroxy radical pool parameterisation: In a system with *n* peroxy radicals, there are *n* self-reactions and ½*n*(*n*-1) cross reactions i.e. ½*n*(*n*+1) permutation reactions in total. In view of the large number of RO_2 radicals generated in a detailed chemical mechanism, these reactions cannot therefore be represented explicitly. The MCM has traditionally applied a very simplified approach, in which each peroxy radical is assumed to react with all other peroxy radicals (i.e. the peroxy radical "pool") at a single, collective rate (Jenkin et al., 1997). This is achieved by defining a parameter "$\sum[RO_2]$" which is the sum of the concentrations of all peroxy radicals, excluding HO_2. The collective rate of all the permutation reactions of a particular peroxy radical is then represented by a single pseudo-unimolecular reaction, which has an assigned rate coefficient equal to $k_7 \times \sum[RO_2]$:

$$RO_2 \rightarrow \text{products} \qquad \text{(S7)}$$

The rate coefficient for a given peroxy radical is based on that estimated for the cross-reaction of that peroxy radical with CH_3O_2. This is regarded as a logical choice, because CH_3O_2 is the most abundant organic peroxy radical in the atmosphere (and therefore most commonly the major reaction partner), and also possesses a self-reaction rate coefficient that is in the middle of the range of reported values (see Tables 9 and 10 in the main paper). The updated method, based on the simplified MCM approach, is fully described in Sect. 2.6 of the main paper.

Multi-class peroxy radical pool parameterisation: A similar, but more detailed, approach has traditionally been applied in GECKO-A, in which the peroxy radical population is divided into a number of reactivity classes (Aumont et al., 2005). This requires the inclusion of a pseudo-unimolecular reaction (analogous to reaction (S7)) for reaction of a given peroxy radical with each peroxy radical class. Table S3 shows a series of nine reactivity classes that are considered in the present work, designed to cover the wide range in reported self-reaction reactivity. In seven cases, the class contains a set of peroxy radicals that are expected to possess comparable self-reaction reactivities; with an additional constraint that tertiary radicals are placed in unique classes because of differences in product branching ratios (see below). The remaining two classes contain only a single radical, namely CH_3O_2 and i-$C_3H_7O_2$, which possess distinct reactivities from the other classes. As indicated above, CH_3O_2 is also typically the most abundant organic peroxy radical.

The rate coefficients (in cm^3 $molecule^{-1}$ s^{-1}) for the parameterized permutation reactions of a given peroxy radical with these classes at 298 K are defined as follows:

(i) For reaction of an acyl peroxy radical ($R'C(O)O_2$) with any of the classes 1-9, or the reaction of any peroxy radical with the $R'C(O)O_2$ class (class 9), the following rate coefficient is applied:

$k_{AP} = 2.0 \times 10^{-12} \exp(508/T)$ cm^3 $molecule^{-1}$ s^{-1}

This is based on a value of 1.1×10^{-11} cm^3 $molecule^{-1}$ s^{-1} at 298 K (see Fig. 5 of the main paper), combined with a pre-exponential factor of 2.0×10^{-12} cm^3 $molecule^{-1}$ s^{-1}.

(ii) For all other reactions, except the reactions of CH_3O_2 with itself (class 6) and i-$C_3H_7O_2$ with itself (class 2), the 298 K rate coefficient is calculated as follows:

$k_{RO2(298K)} = f_{RO2} \times 2 \times (k_{RO2RO2} \times k_{298}(R_iO_2+R_iO_2))^{0.5}$

Here, $k_{298}(R_iO_2+R_iO_2)$ is the appropriate class rate coefficient given in Table S3 and k_{RO2RO2} is the 298 K self-reaction rate coefficient for the reacting peroxy radical, estimated as described in Sect. 2.6 of the main paper. As also described in Sect. 2.6, f_{RO2} is a scaling factor that is informed by the correlations of cross-reaction rate coefficients in Fig. 5 of the main paper. In the present extension to the method, it takes a unity value for primary and secondary peroxy radicals reacting with classes 2, 4 and 6-8; and for tertiary peroxy radicals reacting with classes 1, 3 and 5. A value of $f_{RO2} = 2$ is applied for primary and secondary peroxy radicals reacting with classes 1, 3 and 5; and for tertiary peroxy radicals reacting with classes 2, 4 and 6-8. As also indicated in Sect 2.6, the corresponding temperature-dependent rate coefficient, k_{RO2}, is assigned a pre-exponential factor of 1.0 x 10^{-13} cm^3 $molecule^{-1}$ s^{-1}. This results in the following temperature dependent expression,

$$k_{RO2} = 1.0 \times 10^{-13} \exp(-(E_{RO2}/R)/T) \text{ cm}^3 \text{ molecule}^{-1} \text{ s}^{-1}$$

with E_{RO2}/R having a case dependent value of $-298 \times \ln(k_{RO2(298K)}/10^{-13})$, where $k_{RO2(298K)}$ is defined above.

The collective rate of the permutation reactions of a given peroxy radical with each of the classes listed in Table S3 is then represented by a pseudo-unimolecular reaction (reaction (S7)), which has an assigned rate coefficient equal to either $k_{AP} \times \sum[RO_2]_i$ or $k_{RO2} \times \sum[RO_2]_i$ (as outlined above) where $[RO_2]_i$ is the sum of the concentrations of the pool of peroxy radicals in class "i".

Table S3. Peroxy radical reactivity classes and their self-reaction rate coefficients at 298 K, as applied to the calculation of permutation reaction rate coefficients in the multi-class parameterization (see Sect. S4).

Class	Contributing RO_2	$k_{298}(R_iO_2+R_iO_2)$	Comment
		(10^{-14} cm^3 $molecule^{-1}$ s^{-1})	
1	unsubstituted *tert*-RO_2	0.0021	(a),(b)
2	*i*-$C_3H_7O_2$	0.10	(c)
3	*tert*-RO_2 with α- or β- O or N	0.79	(d)
4	$C_2H_5O_2$; unsubstituted *sec*-RO_2;	6.9	(e),(b)
5	*tert*-RO_2 with α- or β- O or N and allyl or benzyl group	10	(f)
6	CH_3O_2	35	(g)
7	unsubstituted *prim*-RO_2; *sec*-RO_2 with α- or β- O or N	110	(h),(b)
8	*prim*-RO_2 with α- or β- O or N; *sec*-RO_2 with α- or β- O or N and allyl or benzyl group	530	(i)
9	R'C(O)O_2	1400	(j)

Comments

[a] Based on Eq. (16) in Sect. 2.6 for tertiary radical with no substituents; [b] The term "unsubstituted" includes corresponding RO_2 containing remote oxygenated groups (i.e. not α- or β-) and/or remote unsaturated linkages (i.e. not allyl or benzyl); [c] Rate coefficient for *i*-$C_3H_7O_2$ in Table 9; [d] Based on Eq. (16) in Sect. 2.6 for tertiary radical with β-hydroxy substituent; [e] Geometric mean of rate coefficient for $C_2H_5O_2$ in Table 9 (7.6 × 10^{-14} cm^3 $molecule^{-1}$ s^{-1}) and rate coefficient based on Eq. (16) in Sect. 2.6 for secondary radical (n_{CON} = 6) with no substituents (6.3 × 10^{-14} cm^3 $molecule^{-1}$ s^{-1}); [f] Based on Eq. (16) in Sect. 2.6 for tertiary radical with β-hydroxy and allyl substituents; [g] Rate coefficient for CH_3O_2 in Table 9; [h] Rate coefficient based on Eq. (16) in Sect. 2.6 for primary radical (n_{CON} = 5) with no substituents (1.07 × 10^{-12} cm^3 $molecule^{-1}$ s^{-1}); and for secondary radical (n_{CON} = 7) with β-hydroxy substituent (1.17 × 10^{-12} cm^3 $molecule^{-1}$ s^{-1}); [i] Geometric mean of rate coefficients based on Eq. (16) in Sect. 2.6 for primary radical (n_{CON} = 6) with β-hydroxy substituent (6.1 × 10^{-12} cm^3 $molecule^{-1}$ s^{-1}); and for secondary radical (n_{CON} = 8) with β-hydroxy and allyl substituents (4.6 × 10^{-12} cm^3 $molecule^{-1}$ s^{-1}); [j] Based on data for acyl peroxy radicals in Table 10.

Table S4. Branching ratios assigned to parameterized permutation reactions of the reagent RO_2 with the reactivity classes shown (see Sect. S4).

RO_2	Reactivity class	Channel branching ratio			Comment
		k_{7a}/k_7	k_{7b}/k_7	k_{7c}/k_7	
CH_3O_2	6 (i.e. CH_3O_2)	$7.2 \times \exp(-885/T)$	$(1-k_{7a}/k_7)/2$	$(1-k_{7a}/k_7)/2$	(a)
	2, 4, 7, 8	0.6	0.2	0.2	(b)
	1, 3, 5, 9	0.8	0.2	-	(c),(d)
Primary and secondary	2, 4, 6-8	0.6	0.2	0.2	(b)
	1, 3, 5, 9	0.8	0.2	-	(c),(d)
Tertiary and acyl	2, 4, 6-8	0.8	-	0.2	(c),(e)
	1, 3, 5, 9	1.0	-	-	(f)

Comments

[a] Based on IUPAC recommendation for the CH_3O_2 self-reaction (http://iupac.pole-ether.fr/). Temperature-dependent channel rate coefficients can alternatively be applied, as described in Sect. S5; [b] Based on a rounded mean of the reported 298 K branching ratios for the self-reactions of $C_2H_5O_2$, i-$C_3H_7O_2$, $HOCH_2CH_2O_2$, $(CH_3)_2C(OH)CH_2O_2$, $CH_3C(O)CH_2O_2$, $CH_3OCH_2O_2$, and $C_6H_5CH_2O_2$ based on IUPAC recommendations (http://iupac.pole-ether.fr/); *neo*-$C_5H_{11}O_2$, c-$C_6H_{11}O_2$ and CH_2=$CHCH_2O_2$ based on Lightfoot et al. (1990), Rowley et al. (1991), Jenkin et al. (1993) and Boyd et al. (1996); and for the self- and cross- reactions of primary and secondary RO_2 formed from reactions of OH with conjugated dienes (Jenkin et al., 1998); [c] Based on a rounded mean of the reported 298 K branching ratios for the following cross-reactions: $CH_3C(O)O_2$ + CH_3O_2, $C_2H_5C(O)O_2$ + $C_2H_5O_2$ and $CH_3C(O)O_2$ + $CH_3C(O)CH_2O_2$, based on IUPAC recommendations (http://iupac.pole-ether.fr/); and $HOCH_2C(CH_3)(O_2)C(CH_3)$=$CH_2$ + $HOCH_2C(CH_3)$=$C(CH_3)CH_2O_2$ formed from reaction of OH with 2,3-dimethyl-buta-1,3-diene (Jenkin et al., 1998); [d] Channel (S7c) is unavailable because peroxy radicals in these reactivity classes do not possess α- H atoms; [e] Channel (S7b) is unavailable because reagent RO_2 does not possess α- H atom; [f] Channels (S7b) and (S7c) are unavailable because neither reagent RO_2 nor peroxy radicals in these reactivity classes possess α- H atoms.

In the specific cases of CH_3O_2 reacting with itself (class 6) and *i*-$C_3H_7O_2$ reacting with itself (class 2) the applied rate coefficients (k_{CH3O2} and $k_{i\text{-}C3H7O2}$) are twice the self-reaction rate coefficients given in Table 9 of the main paper,

$$k_{CH3O2} = 2.06 \times 10^{-13} \exp(365/T) \text{ cm}^3 \text{ molecule}^{-1} \text{ s}^{-1}$$

$$k_{i\text{-}C3H7O2} = 3.2 \times 10^{-12} \exp(-2200/T) \text{ cm}^3 \text{ molecule}^{-1} \text{ s}^{-1}$$

with the respective pseudo-unimolecular reaction rate coefficients equal to $k_{CH3O2} \times [CH_3O_2]$ and $k_{i\text{-}C3H7O2} \times [\,i\text{-}C_3H_7O_2]$. This preserves the recommended self-reaction rate coefficient in each case. Alternatively, the CH_3O_2 + CH_3O_2 and *i*-$C_3H_7O_2$ + i-$C_3H_7O_2$ reactions can be represented explicitly.

Up to three product channels are represented for each reaction (see Sect. 2.6), these being the pseudo-unimolecular representation of the self-reaction channels (S5a) and (S5b) and the cross-reaction channels (S6a)-(S6c):

$$RO_2 \rightarrow RO \qquad \text{(S7a)}$$

$$\rightarrow R_{\text{-}H}O \qquad \text{(S7b)}$$

$$\rightarrow ROH \qquad \text{(S7c)}$$

The assigned branching ratios depend on both the structure of the reagent RO_2 and on the reactivity class of peroxy radicals it is reacting with, as summarized in Table S4.

As discussed above in Sect. S4, the use of temperature-dependent branching ratios in mechanism application can result in computational difficulties, such that individual channel rate coefficients may provide a more practical alternative. The IUPAC Task Group also recommends the following individual channel rate coefficients for the self-reaction of CH_3O_2 over the temperature range 220-330 K, which can be used in conjunction with explicit representation of the CH_3O_2 self-reaction:

$k_{5a\ (CH3O2)} = 7.4 \times 10^{-13} \exp(-520/T)$ cm^3 molecule^{-1} s^{-1}

$k_{5b\ (CH3O2)} = (1.03 \times 10^{-13} \exp(365/T)) – (7.4 \times 10^{-13} \exp(-520/T))$ cm^3 molecule^{-1} s^{-1}

For the parameterized representation of the CH_3O_2 self-reaction (and CH_3O_2 reacting with the peroxy radical pool in the single-class method), the following channel rate coefficient expressions can similarly be applied,

$k_{7a\ (CH3O2)} = 1.48 \times 10^{-12} \exp(-520/T)$ cm^3 molecule^{-1} s^{-1}

$k_{7b\ (CH3O2)} = k_{7c\ (CH3O2)} = (1.03 \times 10^{-13} \exp(365/T)) – (7.4 \times 10^{-13} \exp(-520/T))$ cm^3 molecule^{-1} s^{-1}

leading to overall rate coefficients that are factor of two greater than those above.

Example calculations of k_{RO2RO2} and k_{RO2}: The methods for calculating the self-reaction rate coefficient (k_{RO2RO2}) and the parameterized permutation reaction rate coefficient (k_{RO2}) are illustrated below, using the peroxy radicals formed from the sequential addition of OH and O_2 to isoprene as examples. The presented calculations of k_{RO2} specifically consider the reactions with CH_3O_2, such that each resultant value is appropriate for the single reaction in single-class method (as traditionally used with the MCM), or for reaction with reactivity class 6 in the multi-class method (as traditionally used with GECKO-A).

Example A: $HOCH_2C(CH_3)(O_2)CH=CH_2$

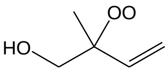

Tertiary peroxy radical:

$n_{CON} = 6$

$k°_{RO2RO2(tert)} = 2.1 \times 10^{-17}$ cm^3 molecule^{-1} s^{-1} (equation (15))

$f_{RO2} = 2$

Substituents (see Table 12 for factors):

β-hydroxy: $\alpha_1 = 8.0 \times 10^{-5}$, $\beta_1 = 0.4$

Allyl (alk-2-enyl): $\alpha_2 = 4.0 \times 10^{-2}$; $\beta_2 = 0.15$

$\alpha = (\alpha_1 \times \alpha_2) = 3.2 \times 10^{-6}$

$\beta = (\beta_1 + \beta_2) = 0.55$

$\mathbf{k_{RO2RO2}} = \alpha \times (k°_{RO2RO2(tert)})^{1-\beta}$ (equation (16))

$= 3.2 \times 10^{-6} \times (2.1 \times 10^{-17})^{0.45} = \mathbf{1.00 \times 10^{-13}}$ cm^3 molecule^{-1} s^{-1}

$k_{RO2(298K)} = f_{RO2} \times 2 \times (k_{RO2RO2} \text{ x } k_{298}(CH_3O_2 + CH_3O_2))^{0.5}$ (equation (18))

$= 2 \times 2 \times (1.00 \times 10^{-13} \times 3.5 \text{ x } 10^{-13})^{0.5} = 7.48 \times 10^{-13}$ cm^3 molecule^{-1} s^{-1}

$k_{RO2} = 1.0 \times 10^{-13} \exp(-(E_{RO2}/R)/T)$ cm^3 molecule^{-1} s^{-1} (equation (20))

$(E_{RO2}/R) = -298 \times \ln(k_{RO2(298\ K)}/10^{-13}) = -600$ K

leading to: $\mathbf{k_{RO2} = 1.0 \times 10^{-13} \exp(600/T)}$ cm^3 molecule^{-1} s^{-1}

<u>Example B</u>: (*E*- and *Z*-) $HOCH_2C(CH_3)=CHCH_2O_2$ and (*E*- and *Z*-) $HOCH_2CH=C(CH_3)CH_2O_2$

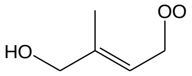

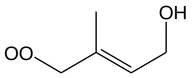

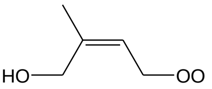

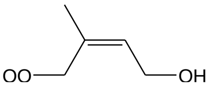

Primary peroxy radical:

$n_{CON} = 6$

$k°_{RO2RO2(prim)} = 1.39 \times 10^{-12}$ cm^3 molecule^{-1} s^{-1} (equation (14))

$f_{RO2} = 1$

Substituents (see Table 12 for factors):

δ-hydroxy: $\alpha_1 = 1.0$, $\beta_1 = 0.0$

Allyl (alk-2-enyl): $\alpha_2 = 4.0 \times 10^{-2}$; $\beta_2 = 0.15$

$\alpha = (\alpha_1 \times \alpha_2) = 4.0 \times 10^{-2}$

$\beta = (\beta_1 + \beta_2) = 0.15$

$\boldsymbol{k}_{\mathbf{RO2RO2}} = \alpha \times (k°_{RO2RO2(prim)})^{1-\beta}$ (equation (16))

$= 4.0 \times 10^{-2} \times (1.39 \times 10^{-12})^{0.85} = \mathbf{3.34 \times 10^{-12}}$ cm^3 molecule^{-1} s^{-1}

$k_{RO2(298K)} = f_{RO2} \times 2 \times (k_{RO2RO2} \times k_{298}(CH_3O_2 + CH_3O_2))^{0.5}$ (equation (18))

$= 1 \times 2 \times (3.34 \times 10^{-12} \times 3.5 \text{ x } 10^{-13})^{0.5} = 2.16 \times 10^{-12}$ cm^3 molecule^{-1} s^{-1}

$k_{RO2} = 1.0 \times 10^{-13} \exp(-(E_{RO2}/R)/T)$ cm^3 molecule^{-1} s^{-1} (equation (20))

$(E_{RO2}/R) = -298 \times \ln(k_{RO2(298 K)}/10^{-13}) = -916$ K

<u>leading to</u>: $\boldsymbol{k}_{\mathbf{RO2}} \mathbf{= 1.0 \times 10^{-13} \exp(916/T)}$ cm^3 molecule^{-1} s^{-1}

<u>Example C</u>: $HOCH_2CH(O_2)C(CH_3)=CH_2$

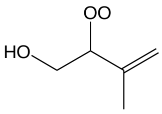

Secondary peroxy radical:

$n_{CON} = 6$

$k°_{RO2RO2(sec)} = 6.31 \times 10^{-14}$ cm^3 molecule^{-1} s^{-1} (equation (13))

$f_{RO2} = 1$

Substituents (see Table 12 for factors):

β-hydroxy: $\alpha_1 = 8.0 \times 10^{-5}$, $\beta_1 = 0.4$

Allyl (alk-2-enyl): $\alpha_2 = 4.0 \times 10^{-2}$; $\beta_2 = 0.15$

$\alpha = (\alpha_1 \times \alpha_2) = 3.2 \times 10^{-6}$

$\beta = (\beta_1 + \beta_2) = 0.55$

$\boldsymbol{k}_{\mathbf{RO2RO2}} = \alpha \times (k°_{\mathrm{RO2RO2(sec)}})^{1-\beta}$ (equation (16))

$= 3.2 \times 10^{-6} \times (6.31 \times 10^{-14})^{0.45} = \mathbf{3.67 \times 10^{-12}}$ cm^3 molecule^{-1} s^{-1}

$k_{\mathrm{RO2(298K)}} = f_{\mathrm{RO2}} \times 2 \times (k_{\mathrm{RO2RO2}} \times k_{298}(\mathrm{CH_3O_2 + CH_3O_2}))^{0.5}$ (equation (18))

$= 1 \times 2 \times (3.67 \text{ x } 10^{-12} \times 3.5 \text{ x } 10^{-13})^{0.5} = 2.27 \times 10^{-12}$ cm^3 molecule^{-1} s^{-1}

$k_{\mathrm{RO2}} = 1.0 \times 10^{-13} \exp(-(\mathrm{E_{RO2}/R})/\mathrm{T})$ cm^3 molecule^{-1} s^{-1} (equation (20))

$(\mathrm{E_{RO2}/R}) = -298 \text{ x } \ln(k_{\mathrm{RO2(298\,K)}}/10^{-13}) = -930$ K

leading to: $\boldsymbol{k}_{\mathbf{RO2}} \mathbf{= 1.0 \times 10^{-13} \exp(930/T)}$ cm^3 molecule^{-1} s^{-1}

Example D: $\mathbf{CH_2{=}C(CH_3)CH(OH)CH_2O_2}$

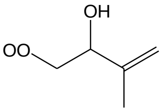

Primary peroxy radical:

$n_{\mathrm{CON}} = 6$

$k°_{\mathrm{RO2RO2(prim)}} = 1.39 \times 10^{-12}$ cm^3 molecule^{-1} s^{-1} (equation (14))

$f_{\mathrm{RO2}} = 1$

Substituents (see Table 12 for factors):

β-hydroxy:	$\alpha_1 = 8.0 \times 10^{-5}$, $\beta_1 = 0.4$
Alk-3-enyl):	$\alpha_2 = 1.0$; $\beta_2 = 0.0$

$\alpha = (\alpha_1 \times \alpha_2) = 8.0 \times 10^{-5}$

$\beta = (\beta_1 + \beta_2) = 0.4$

$\boldsymbol{k}_{\mathbf{RO2RO2}} = \alpha \times (k°_{\mathrm{RO2RO2(prim)}})^{1-\beta}$ (equation (16))

$= 8.0 \times 10^{-5} \times (1.39 \times 10^{-12})^{0.6} = \mathbf{6.15 \times 10^{-12}}$ cm^3 molecule^{-1} s^{-1}

$k_{\mathrm{RO2(298K)}} = f_{\mathrm{RO2}} \times (k_{\mathrm{RO2RO2}} \times k_{298}(\mathrm{CH_3O_2 + CH_3O_2}))^{0.5}$ (equation (18))

$= 1 \times 2 \times (6.15 \times 10^{-12} \times 3.5 \text{ x } 10^{-13})^{0.5} = 2.93 \times 10^{-12}$ cm^3 molecule^{-1} s^{-1}

$k_{\mathrm{RO2}} = 1.0 \times 10^{-13} \exp(-(\mathrm{E_{RO2}/R})/\mathrm{T})$ cm^3 molecule^{-1} s^{-1} (equation (20))

$(\mathrm{E_{RO2}/R}) = -298 \times \ln(k_{\mathrm{RO2(298\,K)}}/10^{-13}) = -1007$ K

leading to: $\boldsymbol{k}_{\mathbf{RO2}} \mathbf{= 1.0 \times 10^{-13} \exp(1007/T)}$ cm^3 molecule^{-1} s^{-1}

S6 1,6 H-shift reactions of isoprene RO_2

As discussed in Sect. 3.2 of the main paper, species-specific rate coefficients are applied to the 1,6 hydroxyalkyl H-shift reactions of (*Z*)-$CH_2(OH)C(CH_3)=CHCH_2O_2$ and (*Z*)-$CH_2(OH)CH=C(CH_3)CH_2O_2$, formed from the sequential addition of OH and O_2 to isoprene. The values are given in Table S5. These are taken from MCM v3.3.1 (Jenkin et al., 2015) and are based on the calculations of Peeters et al. (2014), optimized to the observations of Crounse et al. (2011; 2014). It is noted that Wennberg et al. (2018) have recently reported empirically optimized rate expressions (see Table S5 comments) that give values of k_{298K} that are about a factor of three greater in each case. In conjunction with the parameters applied to the reversible addition of O_2 to the precursor OH-isoprene adducts, however, the two studies provide consistent phenomenological bulk isomerisation rates for typical atmospheric conditions. The MCM v3.3.1 expressions are retained in the present work, because they are compatible with the parameters assigned to reversible OH-isoprene adduct + O_2 reactions given in Jenkin et al. (2018a).

Table S5. Rate coefficients assigned to selected H-shift isomerization reactions of peroxy radicals.

Radical	Product	*k(T)*	$k_{298\,K}$	Comment
		(s^{-1})	(s^{-1})	
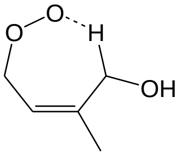	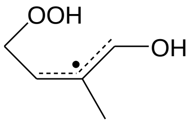	$8.14 \times 10^9 \exp(-8591/T) \times \exp(10^8/T^3)$	0.108	(a)
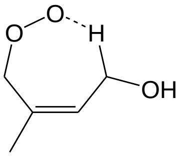	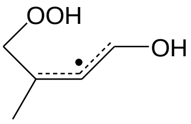	$2.20 \times 10^{10} \exp(-8174/T) \times \exp(10^8/T^3)$	1.18	(b)

Comments

[a] The rate coefficient for (*Z*)-$CH_2(OH)C(CH_3)=CHCH_2O_2$ is taken from MCM v3.3.1 (where it is denoted CISOPAO2). The value is based on the calculations of Peeters et al. (2014) (where it is denoted *Z*-1-OH-4-OO), optimized to the observations of Crounse et al. (2011; 2014). Wennberg et al. (2018) have more recently reported an empirically optimized expression, $k(T) = 5.04 \times 10^{15} \exp(-12200/T) \times \exp(10^8/T^3)$. [b] The rate coefficient for (*Z*)-$CH_2(OH)CH=C(CH_3)CH_2O_2$, is taken from MCM v3.3.1 (where it is denoted CISOPCO2). The value is based on the calculations of Peeters et al. (2014) (where it is denoted *Z*-4-OH-1-OO), optimized to the observations of Crounse et al. (2011; 2014). Wennberg et al. (2018) have more recently reported an empirically optimized expression, $k(T) = 2.22 \times 10^9 \exp(-7160/T) \times \exp(10^8/T^3)$.

References

Anglada, J. M. and Solé, A.: Tropospheric oxidation of methyl hydrotrioxide (CH_3OOOH) by hydroxyl radical, Phys. Chem. Chem. Phys., 20, 27406-27417, 2018.

Arey, J., Aschmann, S. M., Kwok, E. S. C., and Atkinson, R.: Alkyl nitrate, hydroxyalkyl nitrate, and hydroxycarbonyl formation from the NO_x–air photooxidations of C_5–C_8 n-alkanes, J. Phys. Chem. A, 105, 1020–1027, doi:10.1021/jp003292z, 2001.

Assaf, E., Schoemaecker, C., Vereecken, L. and Fittschen, C.: Experimental and theoretical investigation of the reaction of RO_2 radicals with OH radicals: Dependence of the HO_2 yield on the size of the alkyl group, Int. J. Chem. Kinet., 50, 670-680, 2018.

Aumont, B., Szopa, S., and Madronich, S.: Modelling the evolution of organic carbon during its gas-phase tropospheric oxidation: development of an explicit model based on a self generating approach, Atmos. Chem. Phys., 5, 2497–2517, 2005.

Boyd, A. A., Noziere, B. and Lesclaux, R.: Kinetic studies of the allylperoxyl radical self-reaction and reaction with HO_2, Chem. Soc., Faraday Trans., 92 (2), 201-206, 1996a.

Calvert, J. G., Orlando, J. J., Stockwell, W. R. and Wallington, T. J.: The mechanisms of reactions influencing atmospheric ozone, Oxford University Press, Oxford. ISBN 978-0-19-023301-0, 2015.

Caralp, F., and Forst, W.: Chemical activation in unimolecular reactions of some unsubstituted alkoxy radicals, Phys. Chem. Chem. Phys., 5, 4653–4655, 2003.

Caralp, F., Forst, W., and Rayez, M. T.: Chemical activation in OH radical-oxidation of 1-n-alkenes, Phys. Chem. Chem. Phys., 5, 476–486, 2003.

Caralp, F., Forst, W., and Bergeat, A.: A new look at reactions of 2-butoxy and 1-butoxy radicals in the presence of oxygen, Phys. Chem. Chem. Phys., 10, 5746–5753, 2008.

Cassanelli, P., Johnson, D., and Cox, R. A.: A temperature-dependent relative-rate study of the OH initiated oxidation of n-butane: The kinetics of the reactions of the 1- and 2-butoxy radicals, Phys. Chem. Chem. Phys., 7, 3702-3710, 2005.

Christensen, L. K., Ball, J. C., and Wallington, T. J.: Atmospheric oxidation mechanism of methyl acetate, J. Phys. Chem. A, 104, 345-351, 2000.

Crounse, J. D., Paulot, F., Kjaergaard, H. G., and Wennberg, P. O.: Peroxy radical isomerization in the oxidation of isoprene, Phys. Chem. Chem. Phys., 13, 13607–13613, 2011.

Crounse, J. D., Teng, A., and Wennberg, P. O.: Experimental constraints on the distribution and fate of peroxy radicals formed in reactions of isoprene + OH + O2, presented at Atmospheric Chemical Mechanisms: Simple Models – Real World Complexities, University of California, Davis, USA, 10–12 December 2014.

Dillon, T. J. and Crowley, J. N.: Direct detection of OH formation in the reactions of HO_2 with $CH_3C(O)O_2$ and other substituted peroxy radicals, Atmos. Chem. Phys., 8, 4877–4889, doi:10.5194/acp-8-4877-2008, 2008.

Elrod, M. J.: Kinetics study of the aromatic bicyclic peroxy radical + NO Reaction: overall rate constant and nitrate product yield measurements, J. Phys. Chem. A, 115, 8125–8130, 2011.

Geiger, H. et al.: Chemical mechanism development: laboratory studies and model applications, J. Atmos. Chem., 42, 323–357, 2002.

Groß, C. B. M., Dillon, T. J., Schuster, G., Lelieveld, J., and Crowley, J. N.: Direct kinetic study of OH and O_3 formation in the reaction of $CH_3C(O)O_2$ with HO_2, J. Phys. Chem. A, 118, 974–985, doi:10.1021/jp412380z, 2014.

Hasson, A. S., Tyndall, G. S., and Orlando, J. J.: A product yield study of the reaction of HO_2 Radicals with ethyl peroxy ($CH_3CH_2O_2$), acetyl peroxy ($CH_3C(O)O_2$), and acetonyl peroxy ($CH_3C(O)CH_2O_2$) radicals, J. Phys. Chem. A, 108, 5979–5989, 2004.

Hasson, A. S., Kuwata, K. T., Arroyo, M. C., and Petersen, E. B.: Theoretical studies of the reaction of hydroperoxy radicals (HO_2) with ethyl peroxy ($CH_3CH_2O_2$), acetyl peroxy ($CH_3C(O)O_2$), and acetonyl peroxy ($CH_3C(O)CH_2O_2$) radicals, J. Photochem. Photobiol. A, 176, 218-230, 2005.

Horie, O. and Moortgat, G. K.: Reactions of $CH_3C(O)O_2$ radicals with CH_3O_2 and HO_2 between 263 K and 333 K, J. Chem. Soc. Faraday Trans., 88, 3305, 1992.

Jenkin, M. E., Murrells, T. P., Shalliker, S. J., and Hayman, G. D.: Kinetics and product study of the self-reactions of allyl and allyl peroxy radicals at 296 K, J. Chem. Soc. Faraday Trans., 89, 433–446, 1993.

Jenkin, M. E., Saunders, S. M. and Pilling M. J.: The tropospheric degradation of volatile organic compounds: a protocol for mechanism development, Atmos. Environ., 31(1), 81-104, 1997.

Jenkin, M. E., Boyd, A. A., and Lesclaux, R.: Peroxy radical kinetics resulting from the OH-initiated oxidation of 1,3-butadiene, 2,3-dimethyl-1,3-butadiene and isoprene, J. Atmos. Chem., 29, 267–298, 1998.

Jenkin, M. E., Hurley, M. D., and Wallington, T. J.: Investigation of the radical product channel of the $CH_3C(O)O_2$ + HO_2 reaction in the gas phase, Phys. Chem. Chem. Phys., 9, 3149–3162, 2007.

Jenkin, M. E., Young, J. C., and Rickard, A. R.: The MCM v3.3.1 degradation scheme for isoprene, Atmos. Chem. Phys., 15, 11433-11459, doi:10.5194/acp-15-11433-2015, 2015.

Jenkin, M. E., Valorso, R., Aumont, B., Rickard, A. R., and Wallington, T. J.: Estimation of rate coefficients and branching ratios for gas-phase reactions of OH with aliphatic organic compounds for use in automated mechanism construction, Atmos. Chem. Phys., 18, 9297-9328, https://doi.org/10.5194/acp-18-9297-2018, 2018a.

Jenkin, M. E., Valorso, R., Aumont, B., Rickard, A. R., and Wallington, T. J.: Estimation of rate coefficients and branching ratios for gas-phase reactions of OH with aromatic organic compounds for use in automated mechanism construction, Atmos. Chem. Phys., 18, 9329-9349, https://doi.org/10.5194/acp-18-9329-2018, 2018b.

Libuda, H. G., Shestakov, O., Theloke, J., and Zabel, F.: Relative-rate study of thermal decomposition of the 2-butoxyl radical in the temperature range 280–313 K, Phys. Chem. Chem. Phys., 4, 2579–2586, 2002.

Lightfoot, P. D., Cox, R. A., Crowley, J. N., Destriau, M., Hayman, G. D., Jenkin, M. E., Moortgat, G. K., and Zabel, F.: Organic peroxy radicals : kinetics, spectroscopy and tropospheric chemistry, Atmos. Environ., 26A, 1805–1964, 1992.

Müller, J. F., Liu, Z., Nguyen, V. S., Stavrakou, T., Harvey, J. N., and Peeters, J.: The reaction of methyl peroxy and hydroxyl radicals as a major source of atmospheric methanol, Nat. Commun., 7, 2016.

Niki, H., Maker, P. D., Savage, C. M. and Breitenbach, L. P.: FTIR study of the kinetics and mechanism for Cl-atom-initiated reactions of acetaldehyde, J. Phys. Chem. 89, 588-591, 1985.

Orlando, J. J. and Tyndall, G. S.: Laboratory studies of organic peroxy radical chemistry: an overview with emphasis on recent issues of atmospheric significance, Chem. Soc. Rev., 41, 6294–6317, 2012.

Orlando, J. J., Tyndall, G. S., Bilde, M., Ferronato, C., Wallington, T. J., Vereecken, L., and Peeters, J.: Laboratory and theoretical study of the oxy radicals in the OH- and Cl-initiated oxidation of ethene, J. Phys. Chem. A, 102, 8116-8123, 1998.

Orlando, J. J., Tyndall, G. S., Vereecken, L., and Peeters, J.: The atmospheric chemistry of the acetonoxy radical, J. Phys. Chem. A, 104, 11578-11588, 2000.

Orlando, J. J., Tyndall, G. S. and Wallington, T. J.: The atmospheric chemistry of alkoxy radicals, Chem. Rev., 103, 4657-4689, 2003.

Peeters, J., Müller, J.-F., Stavrakou, T., and Nguyen, V. S.: Hydroxyl radical recycling in isoprene oxidation driven by hydrogen bonding and hydrogen tunneling: the upgraded LIM1 mechanism, J. Phys. Chem. A, 118, 8625–8643, 2014.

Praske, E., Crounse, J. D., Bates, K. H., Kurtén, T., Kjaergaard, H. G. and Wennberg, P. O.: Atmospheric fate of methyl vinyl ketone: peroxy radical reactions with NO and HO_2, J. Phys. Chem. A, 119(19), 4562-4572, 2015.

Rowley, D. M., Lightfoot, P. D., Lesclaux, R. and Wallington, T. J.: UV Absorption spectrum and self-reaction of cyclohexylperoxy radicals, J. Chem. Soc. Faraday Trans., 87(19), 3221-3226, 1991.

Vereecken, L., and Peeters, J.: Theoretical investigation of the role of intramolecular hydrogen bonding in β-hydroxyethoxy and β -hydroxyethylperoxy radicals in the tropospheric oxidation of ethene, J. Phys. Chem. A, 103, 1768-1775, 1999.

Vereecken, L., Peeters, J., Orlando, J. J., Tyndall, G. S., and Ferronato, C.: Decomposition of β-hydroxypropoxy radicals in the OH-initiated oxidation of propene. A theoretical and experimental study J. Phys. Chem. A, 103, 4693-4702, 1999.

Wallington, T. J., Hurley, M. D., Maurer, T., Barnes, I., Becker, K. H., Tyndall, G. S., Orlando, J. J., Pimentel, A. S. and Bilde, M.: Atmospheric oxidation mechanism of methyl formate, J. Phys. Chem. A, 105, 5146-5154, 2001.

Wennberg, P. O., Bates, K. H., Crounse, J. D., Dodson, L. G., McVay, R. C., Mertens, L. A., Nguyen, T. B., Praske, E., Schwantes, R. H., Smarte, M. D., St Clair, J. M., Teng A. P., Zhang, X. and Seinfeld, J. H.: Gas-phase reactions of isoprene and its major oxidation products, Chem. Rev., 118 (7), 3337-3390, 2018.

Winiberg, F. A. F., Dillon, T. J., Orr, S. C., Groß, C. B. M., Bejan, I., Brumby, C. A., Evans, M. J., Smith, S. C., Heard, D. E., and Seakins, P. W.: Direct measurements of OH and other product yields from the HO_2 + $CH_3C(O)O_2$ reaction, Atmos. Chem. Phys., 16, 4023-4042, doi:10.5194/acp-16-4023-2016, 2016.